Plasmon excitation by charged particles moving near a solid surface

C. Denton
Departamento de Física Aplicada, Universidad de Alicante, Apt. 99, E-03080 Alicante, Spain

J. L. Gervasoni,* R. O. Barrachina,* and N. R. Arista
Comisión Nacional de Energía Atómica, Centro Atómico Bariloche e Instituto Balseiro,† 8400 Bariloche, Argentina
(Received 30 December 1997)

The interaction of fast charged particles with a semi-infinite medium is described using both quantum-mechanical and semiclassical dielectric formulations. We consider the coupling with bulk and surface excitations for arbitrary trajectories of the particle and apply the solutions to several cases of special interest. Interference effects in bulk and surface excitations for some particular trajectories are described. We analyze in detail the process of reflection-electron-energy-loss spectroscopy, obtaining results for the probabilities of multiple bulk- and surface-plasmon excitations. The calculations are compared with available experimental results, showing a good description of the angular dependence of the excitation phenomenon.
[S1050-2947(98)00506-X]

PACS number(s): 79.20.Rf, 34.50.Bw

I. INTRODUCTION

Plasmon excitation, both at the surface and in the bulk of the material, is one of the most relevant processes in the interaction of swift charged particles with solid samples. These excitations are of interest in studies of electron and ion interactions with surfaces or thin solid foils, and in reflection-electron-energy-loss spectroscopy (REELS) of solids [1,2].

The theoretical description of these processes is usually based either on the dielectric formulation [3–7], or in the quantized plasmon-field approach [8–10]. Both pictures provide valuable views of the process and serve to illustrate the classical and quantum aspects of the interactions. Several calculations based on these methods have been made, but mostly for particles with normal or grazing incidence trajectories. Recent work by Yubero and co-workers [11,12], using the dielectric formulation, incorporates the full dielectric properties of the solid as obtained from optical data, for materials with more complex electronic structure; the model also considers the angular dependence of the process.

The purpose of this work is first to formulate in more general terms the excitations produced by charged particles with arbitrary motion near a solid-vacuum interface, including the case of penetrating trajectories, and second, to apply this description to the important case of reflection-electron-energy-loss experiments. The present study is formulated using both the dielectric description and the quantum representation of bulk- and surface-plasmon excitations.

The paper is organized as follows. First we briefly review the so-called specular-reflection model based on the dielectric formalism (Sec. I) and reformulate the description to incorporate the more general case of particles moving with arbitrary trajectories in the presence of a solid-vacuum interface (Sec. II). Using a semiclassical picture we derive expressions to calculate the average energy loss of the particle due to bulk and surface excitations (Sec. III). In Sec. IV we apply the general expressions to various particular cases of interest, like a single crossing of the surface by a particle with uniform motion, a particle that reverses its motion inside the medium, and a particle being reflected near a metal surface, both for the cases of normal or oblique incidence. In Sec. V we apply the description to the relevant case of REEL experiments, and compare the results with those from Powell's experiments. The main conclusions of this work are indicated in Sec. VI. We include in the Appendix a derivation of the excitation probabilities for bulk and surface plasmons using the quantum formulation. We show the essential agreement of both methods for the case of simple metals, in the plasmon-pole approximation.

II. SPECULAR-REFLECTION MODEL

Let us consider an external charge density $\rho^{\mathrm{ext}}(\mathbf{r},t)$ acting on an interface between a metal ($z<0$) of dielectric function $\varepsilon(k,\omega)$ and the vacuum ($z>0$). Figure 1 illustrates in a

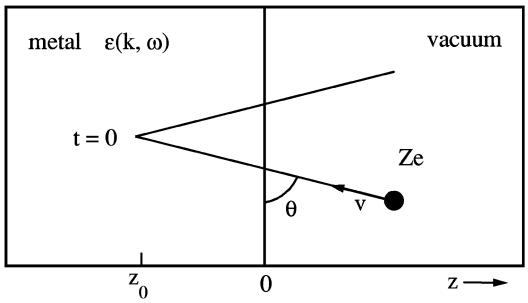

FIG. 1. Illustration of the scattering of a particle in a semi-infinite dielectric medium. This figure corresponds to the case of a particle incident with an angle θ relative to the surface plane, and reflected at a point z_0 inside the medium, as in the case of REEL experiments discussed in Sec. V.

*Also with the Consejo Nacional de Investigaciones Científicas y Técnicas (CONICET), Argentina.

†Comisión Nacional de Energía Atómica (CNEA) and Universidad Nacional de Cuyo (UNC), Argentina.

particular case the geometry of the process. According to the specular-reflection model [4,5], the metal and the vacuum are treated as if they were infinite using symmetrized charged densities,

$$\rho_{\rm metal}=[\rho^{\rm ext}(\mathbf{r},t)+\rho^{\rm ext}(\mathbf{r}',t)][1-\Theta(z)]+\sigma(\mathbf{r},t)\,\delta(z),$$
$$\rho_{\rm vacuum}=[\rho^{\rm ext}(\mathbf{r},t)+\rho^{\rm ext}(\mathbf{r}',t)]\Theta(z)-\sigma(\mathbf{r},t)\,\delta(z), \tag{1}$$

with $\mathbf{r}'=\mathbf{r}-2(\mathbf{r}\cdot\hat{\mathbf{z}})\hat{\mathbf{z}}$. These expressions incorporate the specular image $\rho^{\rm ext}(\mathbf{r}',t)$ of the external density and a surface-charge density σ, which is used to match the potential at the interface. The Heaviside step function $\Theta(z)$ indicates that the charge density in the vacuum does not interact directly with the bulk, and vice versa.

The electric potential is most easily obtained through Poisson's equation in a Fourier transformed space,

$$\phi_{\rm metal}(\mathbf{r},t)=\frac{1}{(2\pi)^4}\int d\mathbf{k}\int d\omega\; e^{i(\mathbf{k}\cdot\mathbf{r}-\omega t)}\phi_{\rm metal}(\mathbf{k},\omega),$$
$$\phi_{\rm vacuum}(\mathbf{r},t)=\frac{1}{(2\pi)^4}\int d\mathbf{k}\int d\omega\; e^{i(\mathbf{k}\cdot\mathbf{r}-\omega t)}\phi_{\rm vacuum}(\mathbf{k},\omega), \tag{2}$$

with

$$\phi_{\rm metal}(\mathbf{k},\omega)=\frac{4\pi}{k^2\varepsilon(k,\omega)}\,\rho_{\rm metal}(\mathbf{k},\omega)$$
$$=\frac{4\pi}{k^2\varepsilon(k,\omega)}\,[\rho^{\rm ext}_{\rm metal}(\mathbf{q}+k_z\hat{\mathbf{z}},\omega)$$
$$+\rho^{\rm ext}_{\rm metal}(\mathbf{q}-k_z\hat{\mathbf{z}},\omega)+\sigma(\mathbf{q},\omega)], \tag{3}$$

$$\phi_{\rm vacuum}(\mathbf{k},\omega)=\frac{4\pi}{k^2}\,\rho_{\rm vacuum}(\mathbf{k},\omega)=\frac{4\pi}{k^2}\,[\rho^{\rm ext}_{\rm vacuum}(\mathbf{q}+k_z\hat{\mathbf{z}},\omega)$$
$$+\rho^{\rm ext}_{\rm vacuum}(\mathbf{q}-k_z\hat{\mathbf{z}},\omega)-\sigma(\mathbf{q},\omega)], \tag{4}$$

with $\rho^{\rm ext}_{\rm metal}(\mathbf{k},\omega)$ and $\rho^{\rm ext}_{\rm vacuum}(\mathbf{k},\omega)$ the Fourier transforms of the *external* charge density $\rho^{\rm ext}$ in each semispace,

$$\rho^{\rm ext}_{\rm metal}(\mathbf{k},\omega)=\int_{z<0}d\mathbf{r}\int_{-\infty}^{\infty}dt\; e^{-i(\mathbf{k}\cdot\mathbf{r}-\omega t)}\rho^{\rm ext}(\mathbf{r},t),$$
$$\rho^{\rm ext}_{\rm vacuum}(\mathbf{k},\omega)=\int_{z>0}d\mathbf{r}\int_{-\infty}^{\infty}dt\; e^{-i(\mathbf{k}\cdot\mathbf{r}-\omega t)}\rho^{\rm ext}(\mathbf{r},t). \tag{5}$$

In the previous equations we have separated the parallel ($\mathbf{q}$) and normal ($k_z\hat{\mathbf{z}}$) components of the wave vector $\mathbf{k}$ relative to the surface ($\mathbf{k}=\mathbf{q}+k_z\hat{\mathbf{z}}$).

Similarly, we get the Fourier transform of the electric field $\mathbf{E}(\mathbf{k},\omega)=-i\mathbf{k}\phi(\mathbf{k},\omega)$. The surface-charge density σ is fixed by the continuity of the potential at the surface, i.e., $\phi_{\rm metal}(\mathbf{r},t)|_{z=0}=\phi_{\rm vacuum}(\mathbf{r},t)|_{z=0}$. This yields

$$\sigma(\mathbf{q},\omega)=\frac{2q}{\pi}\,\frac{\varepsilon_S(q,\omega)}{1+\varepsilon_S(q,\omega)}\int_{-\infty}^{\infty}\frac{dk_z}{k_z^2+q^2}\left(\rho^{\rm ext}_{\rm vacuum}(\mathbf{q}+k_z\hat{\mathbf{z}},\omega)\right.$$
$$\left.-\frac{1}{\varepsilon(\sqrt{k_z^2+q^2},\omega)}\,\rho^{\rm ext}_{\rm metal}(\mathbf{q}+k_z\hat{\mathbf{z}},\omega)\right), \tag{6}$$

where $\varepsilon_S(q,\omega)$ is the surface dielectric function [4,5]

$$\frac{1}{\varepsilon_S(q,\omega)}=\frac{q}{\pi}\int_{-\infty}^{\infty}\frac{dk_z}{k_z^2+q^2}\,\frac{1}{\varepsilon(\sqrt{k_z^2+q^2},\omega)}. \tag{7}$$

These equations provide close expressions for the electric potentials and charge densities at and in both sides of the interface, in terms of the external perturbation $\rho^{\rm ext}(\mathbf{r},t)$ and the dielectric function $\varepsilon(k,\omega)$ of the metal. The integrations in Eqs. (6) and (7) can be treated analytically only for some model dielectric functions. For instance, we can assume that the dielectric function depends on k only through its component q parallel to the surface, i.e., $\varepsilon(q,\omega)$ (see, for instance, Yubero *et al.* [12]). With this approximation, $\varepsilon_S(q,\omega)=\varepsilon(q,\omega)$, and the surface-charge density $\sigma(\mathbf{q},\omega)$ can be obtained by residue integration,

$$\sigma(\mathbf{q},\omega)=\frac{2\varepsilon(q,\omega)}{1+\varepsilon(q,\omega)}\left[\rho^{\rm ext}_{\rm vacuum}(\mathbf{q}-iq\hat{\mathbf{z}},\omega)\right.$$
$$\left.-\frac{1}{\varepsilon(q,\omega)}\,\rho^{\rm ext}_{\rm metal}(\mathbf{q}+iq\hat{\mathbf{z}},\omega)\right]. \tag{8}$$

Here we have extended the limits of integration over k_z to infinity, keeping the usual cutoff [10] only in the parallel component of k, namely, at $q=q_c$. The potential $\phi^{\rm ind}(\mathbf{r},t)$ induced in the medium by the external charge density is obtained from Eqs. (3), (4), and (8) by subtracting the vacuum field of the projectile,

$$\phi^{\rm ind}_{\rm metal}(\mathbf{k},\omega)=\phi_{\rm metal}(\mathbf{k},\omega)-\frac{4\pi}{k^2}[\rho^{\rm ext}_{\rm metal}(\mathbf{k},\omega)+\rho^{\rm ext}_{\rm vacuum}(\mathbf{k},\omega)]$$
$$=\frac{4\pi}{k^2}\left\{\frac{1-\varepsilon(q,\omega)}{1+\varepsilon(q,\omega)}\,[\rho^{\rm ext}_{\rm metal}(\mathbf{q}-ik_z\hat{\mathbf{z}},\omega)\right.$$
$$+\rho^{\rm ext}_{\rm vacuum}(\mathbf{q}+ik_z\hat{\mathbf{z}},\omega)]$$
$$+\frac{1-\varepsilon(q,\omega)}{\varepsilon(q,\omega)}\,[\rho^{\rm ext}_{\rm metal}(\mathbf{q}+ik_z\hat{\mathbf{z}},\omega)$$
$$\left.-\rho^{\rm ext}_{\rm metal}(\mathbf{q}-ik_z\hat{\mathbf{z}},\omega)]\right\}, \tag{9}$$

$$\phi^{\rm ind}_{\rm vacuum}(\mathbf{k},\omega)=\phi_{\rm vacuum}(\mathbf{k},\omega)$$
$$-\frac{4\pi}{k^2}[\rho^{\rm ext}_{\rm metal}(\mathbf{k},\omega)+\rho^{\rm ext}_{\rm vacuum}(\mathbf{k},\omega)]$$
$$=\frac{4\pi}{k^2}\,\frac{1-\varepsilon(q,\omega)}{1+\varepsilon(q,\omega)}\,[\rho^{\rm ext}_{\rm metal}(\mathbf{q}+ik_z\hat{\mathbf{z}},\omega)$$
$$+\rho^{\rm ext}_{\rm vacuum}(\mathbf{q}-ik_z\hat{\mathbf{z}},\omega)]. \tag{10}$$

In order to obtain these simplified expressions for the induced potentials we have replaced $\mathbf{q}\pm iq\hat{\mathbf{z}}$ by $\mathbf{q}\pm ik_z\hat{\mathbf{z}}$. This change does not modify the final expressions in coordinate space and makes the previous equations more readable.

The term proportional to $[1-\varepsilon(q,\omega)]/\varepsilon(q,\omega)$ in Eq. (9) is like the one describing the interaction of an external perturbation with an infinite material, except for the presence of the image charge density $\rho^{\rm ext}_{\rm metal}(\mathbf{q}-ik_z\hat{\mathbf{z}},\omega)$. Note also that

this term appears only when the external charge density $\rho^{\text{ext}}(\mathbf{r},t)$ is different from zero inside the material, since that part of $\rho^{\text{ext}}(\mathbf{r},t)$ that occupies the vacuum semispace does not interact directly with the bulk but only with the surface, through the surface-charge density σ. The effect of this interaction is represented by the terms proportional to $(1-\varepsilon)/(1+\varepsilon)$ in the previous equation.

III. CHARGED PARTICLE MOVING IN AN ARBITRARY TRAJECTORY

Let us now study the perturbation produced by a projectile of charge Z moving in the proximity of a solid surface. Previous model calculations by us [13–16] and other authors (see, for instance, the recent work by Yubero *et al.* [12]) have considered some particular trajectories with simple geometries. In this section, we generalize these previous results by analyzing an arbitrary trajectory $\mathbf{R}=\mathbf{R}(t)$, i.e., $\rho^{\text{ext}}(\mathbf{r},t)=Z\delta(\mathbf{r}-\mathbf{R}(t))$. Replacing in Eqs. (9) and (10), we get

$$\phi^{\text{ind}}_{\text{metal}}(\mathbf{k},\omega)=\frac{4\pi}{k^2}Z\int_{-\infty}^{\infty}dt\ e^{i\omega t}e^{-i\mathbf{q}\cdot\mathbf{R}} \times\left\{\frac{1-\varepsilon(q,\omega)}{1+\varepsilon(q,\omega)}[\Theta(\mathbf{R}\cdot\hat{\mathbf{z}})e^{-ik_z\hat{\mathbf{z}}\cdot\mathbf{R}} +\Theta(-\mathbf{R}\cdot\hat{\mathbf{z}})e^{ik_z\hat{\mathbf{z}}\cdot\mathbf{R}}]+\frac{1-\varepsilon(q,\omega)}{\varepsilon(q,\omega)}\Theta(-\hat{\mathbf{z}}\mathbf{R}) \times[e^{-ik_z\hat{\mathbf{z}}\cdot\mathbf{R}}-e^{ik_z\hat{\mathbf{z}}\cdot\mathbf{R}}]\right\}, \tag{11}$$

$$\phi^{\text{ind}}_{\text{vacuum}}(\mathbf{k},\omega)=\frac{4\pi}{k^2}Z\frac{1-\varepsilon(q,\omega)}{1+\varepsilon(q,\omega)}\int_{-\infty}^{\infty}dt\ e^{i\omega t}e^{-i\mathbf{q}\cdot\mathbf{R}} \times[\Theta(\hat{\mathbf{z}}\cdot\mathbf{R})e^{ik_z\hat{\mathbf{z}}\cdot\mathbf{R}}+\Theta(-\hat{\mathbf{z}}\cdot\mathbf{R})e^{-ik_z\hat{\mathbf{z}}\cdot\mathbf{R}}]. \tag{12}$$

We perform an integral in k_z to get the induced potential in coordinate space.

$$\phi^{\text{ind}}_{\text{metal}}(\mathbf{r},\omega)=\frac{Z}{2\pi}\int\frac{d\mathbf{q}}{q}\int_{-\infty}^{\infty}dt\ e^{i\omega t}e^{i\mathbf{q}\cdot(\mathbf{r}-\mathbf{R})} \times\left[\frac{1-\varepsilon(q,\omega)}{1+\varepsilon(q,\omega)}e^{-q(|\hat{\mathbf{z}}\cdot\mathbf{R}|-z)}+\frac{1-\varepsilon(q,\omega)}{\varepsilon(q,\omega)} \times\Theta(-\hat{\mathbf{z}}\cdot\mathbf{R})(e^{-q|\hat{\mathbf{z}}\cdot\mathbf{R}-z|}-e^{-q|\hat{\mathbf{z}}\cdot\mathbf{R}+z|})\right], \tag{13}$$

$$\phi^{\text{ind}}_{\text{vacuum}}(\mathbf{r},\omega)=\frac{Z}{2\pi}\int\frac{d\mathbf{q}}{q}\int_{-\infty}^{\infty}dt\ e^{i\omega t}e^{i\mathbf{q}\cdot(\mathbf{r}-\mathbf{R})} \times\frac{1-\varepsilon(q,\omega)}{1+\varepsilon(q,\omega)}e^{-q(|\hat{\mathbf{z}}\cdot\mathbf{R}|+z)}. \tag{14}$$

Finally, we can join both expressions for $z<0$ and $z>0$ in one single equation,

$$\phi^{\text{ind}}(\mathbf{r},\omega)=\frac{Z}{2\pi}\int\frac{d\mathbf{q}}{q}\int_{-\infty}^{\infty}dt\ e^{i\omega t}e^{i\mathbf{q}\cdot(\mathbf{r}-\mathbf{R})} \times\left[\frac{1-\varepsilon(q,\omega)}{1+\varepsilon(q,\omega)}e^{-q(|\hat{\mathbf{z}}\cdot\mathbf{R}|+|z|)}+\frac{1-\varepsilon(q,\omega)}{\varepsilon(q,\omega)} \times\Theta(-z)\Theta(-\hat{\mathbf{z}}\cdot\mathbf{R})(e^{-q|\hat{\mathbf{z}}\cdot\mathbf{R}-z|}-e^{-q|\hat{\mathbf{z}}\cdot\mathbf{R}+z|})\right], \tag{15}$$

where $\mathbf{R}=\mathbf{R}(t)$.

IV. ENERGY LOSS AND PLASMON EXCITATION

Following the approach of previous authors, we evaluate the energy-loss rate as

$$\frac{dW}{dt}=Z\left.\frac{\partial\phi^{\text{ind}}(\mathbf{r},t)}{\partial t}\right|_{\mathbf{r}=\mathbf{R}(t)} =-i\frac{Z}{2\pi}\int_{-\infty}^{\infty}d\omega\ \omega e^{-i\omega t}\phi^{\text{ind}}(\mathbf{R}(t),\omega). \tag{16}$$

Thus we obtain

$$\frac{dW}{dt}=\left.\frac{dW}{dt}\right|_B+\left.\frac{dW}{dt}\right|_S, \tag{17}$$

where we separate the terms corresponding to bulk- (B) and surface- (S) plasmon excitation,

$$\left.\frac{dW}{dt}\right|_B=-i\frac{Z^2}{4\pi^2}\Theta(-\hat{\mathbf{z}}\cdot\mathbf{R})\int_{-\infty}^{t}dt'\int_{-\infty}^{\infty}d\omega\ \omega e^{i\omega(t'-t)} \times\Theta(-\hat{\mathbf{z}}\cdot\mathbf{R}')\int\frac{d\mathbf{q}}{q}\frac{1-\varepsilon(q,\omega)}{\varepsilon(q,\omega)}e^{i\mathbf{q}\cdot(\mathbf{R}-\mathbf{R}')} \times[e^{-q|\hat{\mathbf{z}}\cdot(\mathbf{R}-\mathbf{R}')|}-e^{-q|\hat{\mathbf{z}}\cdot(\mathbf{R}+\mathbf{R}')|}], \tag{18}$$

$$\left.\frac{dW}{dt}\right|_S=-i\frac{Z^2}{4\pi^2}\int_{-\infty}^{t}dt'\int_{-\infty}^{\infty}d\omega\ \omega e^{i\omega(t'-t)}\int\frac{d\mathbf{q}}{q} \times\frac{1-\varepsilon(q,\omega)}{1+\varepsilon(q,\omega)}e^{i\mathbf{q}\cdot(\mathbf{R}-\mathbf{R}')}e^{-q(|\hat{\mathbf{z}}\cdot\mathbf{R}|+|\hat{\mathbf{z}}\cdot\mathbf{R}'|)}, \tag{19}$$

with $\mathbf{R}=\mathbf{R}(t)$ and $\mathbf{R}'=\mathbf{R}(t')$.

These expressions can be analytically integrated only for some simple models of the dielectric function. Let us consider—for instance—the classical frequency-dependent dielectric function

$$\varepsilon(q,\omega)=1-\frac{\omega_p^2}{\omega(\omega+i\gamma)} \tag{20}$$

as an instructive approximation. $\omega_p=\sqrt{3/r_S^3}$ is the plasma frequency of the medium in atomic units, with r_S the one-electron radius in the electron gas describing the solid; γ is an effective damping rate which accounts for the finite lifetime of the plasmons. Replacing in the previous equations we obtain

$$\left.\frac{dW}{dt}\right|_B = -Z^2\omega_p^2\Theta(-\hat{\mathbf{z}}\cdot\mathbf{R})\int_0^{q_c} dq \int_{-\infty}^{t} dt' e^{-\gamma(t-t')/2} \times\cos[\omega_p(t-t')]J_0(q|\mathbf{R}-\mathbf{R}'|\sin\varphi)\,[e^{-q|\hat{\mathbf{z}}\cdot(\mathbf{R}-\mathbf{R}')|} - e^{-q|\hat{\mathbf{z}}\cdot(\mathbf{R}+\mathbf{R}')|}]\Theta(-\hat{\mathbf{z}}\cdot\mathbf{R}'), \quad (21)$$

$$\left.\frac{dW}{dt}\right|_S = -Z^2\omega_s^2\int_0^{q_c} dq \int_{-\infty}^{t} dt' e^{-\gamma(t-t')/2}\cos[\omega_s(t-t')] \times J_0(q|\mathbf{R}-\mathbf{R}'|\sin\varphi)e^{-q|\hat{\mathbf{z}}\cdot\mathbf{R}|}e^{-q|\hat{\mathbf{z}}\cdot\mathbf{R}'|}, \quad (22)$$

where $J_0(x)$ is the Bessel function of order 0, $\varphi=\varphi(t,t')$ is the angle between $\mathbf{R}-\mathbf{R}'$ and the normal $\hat{\mathbf{z}}$ to the surface, q_c is the usual cutoff in the plasma response function, and $\omega_s = \omega_p/\sqrt{2}$ is the surface-plasmon frequency. This final expression generalizes previous results for simple trajectories.

V. APPLICATIONS

A. Particle traversing a metal surface

As a first illustrative example, let us review the case of a particle of charge Z that crosses the surface in a normal trajectory, $\mathbf{R}(t)=\mathbf{v}t$, which remains undisturbed by the plasmon excitation events. This approximation holds for sufficiently large kinetic energies, namely, $mv^2/2 \gg \hbar\omega_p$. Both cases corresponding to a projectile abandoning or entering the solid are contemplated. The energy-loss rate reads (for $\gamma=0$)

$$\left.\frac{dW}{dt}\right|_B = -\frac{Z^2}{v}\,\omega_p^2\Theta(-\mathbf{v}\cdot\hat{\mathbf{z}}t)[f_{11}(0)+\mathrm{sgn}(t)f_{11}(2\omega_p|t|) - 2\Theta(t)f_{11}(\omega_p|t|)\cos(\omega_p|t|)], \quad (23)$$

$$\left.\frac{dW}{dt}\right|_S = \frac{Z^2}{v}\,\omega_s^2[\mathrm{sgn}(t)f_{11}(2\omega_s|t|) - 2\Theta(t)f_{11}(\omega_s|t|)\cos(\omega_s|t|)]. \quad (24)$$

Here sgn(x) is the signum function, i.e., -1 for $x<0$ and $+1$ for $x\geq 0$. The auxiliary functions $f_{nm}(x)$ are defined as

$$f_{nm}(x) = \int_0^{\xi} dy \frac{y^m}{(1+y^2)^n} e^{-xy} dy, \quad (25)$$

where $\xi = q_c v/\omega_p$ for bulk-plasmon excitations, and $\xi = v q_c/\omega_s$ for surface-plasmon excitations.

In Fig. 2 we show both terms for a projectile of unity charge crossing the surface of aluminum ($\omega_p=0.55$ a.u., $\gamma/\omega_p=0.067$). We see that $dW/dt|_S$ is only important in the vicinity of the surface. It increases when the projectile approaches the interface, reaches a maximum amplitude at exactly $t=0$, and decreases again, showing an oscillatory behavior once the projectile has traversed the surface. Integrating $dW/dt|_S$ in time we get the total energy transferred to the medium in surface-plasmon excitations,

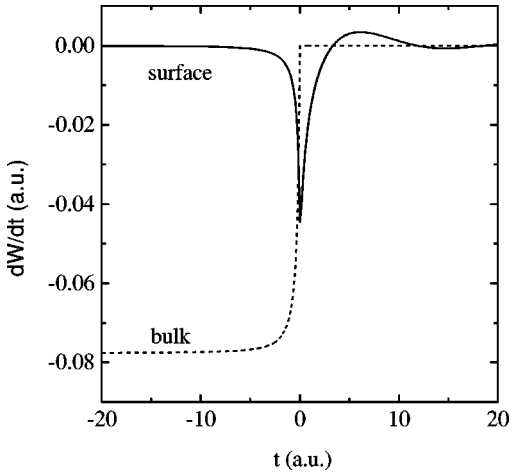

FIG. 2. Energy-loss rate as a function of time t for a particle of unity charge that crosses an aluminum surface in a normal trajectory with velocity $v=10$ a.u. The dashed and solid curves show the contributions from bulk and surface excitations given by Eqs. (23) and (24).

$$\Delta W_S = -\int_{-\infty}^{\infty} dt \left.\frac{dW}{dt}\right|_S = \frac{2Z^2\omega_s}{v} f_{22}(0) = Z^2\frac{\omega_s}{v}\left[\arctan\left(\frac{q_c v}{\omega_s}\right) - \frac{q_c v/\omega_s}{1+(q_c v/\omega_s)^2}\right]. \quad (26)$$

On the other hand, $dW/dt|_B$ is zero while the projectile is in the vacuum semispace ($t>0$). Inside the metal, its first term is independent of time and yields the usual stopping power of a charged projectile in an infinite solid,

$$\left.\frac{dW}{dt}\right|_B = -\frac{Z^2}{v}\,\omega_p^2 f_{11}(0) = -\hbar\omega_p\frac{v}{\lambda_P}, \quad (27)$$

where λ_P is the mean free path for bulk-plasmon excitation, given in this case by

$$\frac{1}{\lambda_P} = \frac{Z^2\omega_p}{\hbar v^2}\ln\sqrt{1+(q_c v/\omega_p)^2}. \quad (28)$$

The ''begrenzung'' term $(Z^2\omega_p^2/v)f_{11}(2\omega_p|t|)$ in Eq. (23) reduces the intensity of the coupling to bulk plasmons in the vicinity of the surface, due to a boundary effect first analyzed by Ritchie [3].

B. Particle reversing its direction of motion inside an infinite solid

Let us now calculate the energy-loss rate by a particle of charge Z and velocity $\mathbf{v}$ that at $t=0$ reverses its direction of motion inside an infinite solid. Even though this example does not use the specular-reflection model, it is illustrative of the effects produced, for instance, by a large-angle elastic scattering. The trajectory is $\mathbf{R}(t)=-\mathbf{v}|t|$. The corresponding external charge density reads

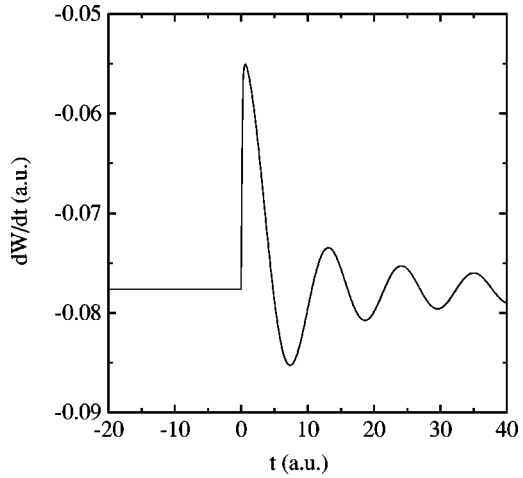

FIG. 3. Energy-loss rate for a particle with velocity $v=10$ a.u. inside aluminum, which at time $t=0$ instantaneously reverses its direction of motion. The stationary energy-loss rate for $t<0$ is the value corresponding to the case of permanent uniform motion.

$$\rho^{\text{ext}}(\mathbf{k},\omega)=Z\left(\frac{i}{\omega+\mathbf{k}\cdot\mathbf{v}+i\eta}-\frac{i}{\omega-\mathbf{k}\cdot\mathbf{v}-i\eta}\right), \tag{29}$$

with $\eta\rightarrow 0^{+}$. Replacing in Eqs. (3) and (16) we obtain

$$\left.\frac{dW}{dt}\right|_B=-\hbar\omega_p\frac{v}{\lambda_P}\{1-\Theta(t)[f_{11}(2\omega_p|t|)-f_{10}(\omega_p|t|)\sin(\omega_p|t|)-f_{11}(\omega_p|t|)\cos(\omega_p|t|)]\}. \tag{30}$$

In Fig. 3 we see that before the collision ($t<0$), the particle loses energy at a constant rate, as given by Eq. (27). For $t>0$, an oscillatory behavior appears. This is due to the fact that the particle traverses again a region where it has excited plasmons in its incoming trajectory. The corresponding induced electric field produces an oscillatory correction to the energy-loss rate which fades away for very large times.

C. Particle reflected near a metal surface with normal incidence

Let us now consider the case of a particle with normal incidence that is reflected at a distance z_0 from a metal-vacuum interface. The trajectory now reads $\mathbf{R}(t)=(v|t|+z_0)\hat{\mathbf{z}}$. The reflection occurs inside or outside the material, depending whether z_0 is negative or positive, respectively. The energy-loss rate becomes

$$\begin{aligned}\left.\frac{dW}{dt}\right|_B=&-\frac{Z^2\omega_p^2}{v}\Theta(-t_o-|t|)\{f_{11}(0)\\&-2f_{11}(\omega_p(|t_o|-|t|))\cos[\omega_p(|t_o|+|t|)]\\&-\mathrm{sgn}(t)f_{11}(2\omega_p(|t_o|-|t|))\\&+2\Theta(t)f_{11}(0)\cos(2\omega_p t)+2\Theta(t)\\&\times[f_{11}(\omega_p(2|t_o|-|t|))-f_{11}(\omega_p t)]\cos(\omega_p t)\},\end{aligned} \tag{31}$$

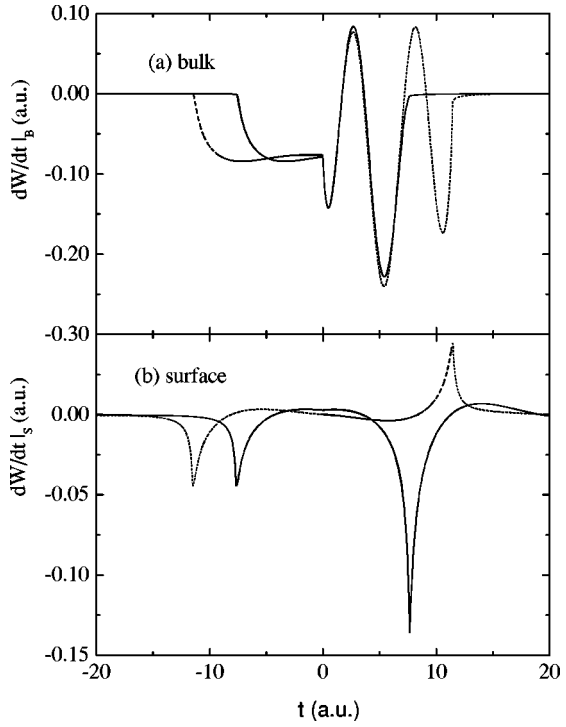

FIG. 4. Energy-loss rate due to the excitation of bulk (a) and surface plasmons (b) for a normally incident particle reflected at time $t=0$ inside aluminum, at a distance z_0 from its surface. The solid and dashed lines correspond to two different reflection distances, $z_0=-\pi v/\omega_s$ (full curve) and $z_0=-3\pi v/2\omega_s$ (dashed curve).

$$\begin{aligned}\left.\frac{dW}{dt}\right|_S=&-\frac{Z^2\omega_s^2}{v}\{-\mathrm{sgn}(t)\mathrm{sgn}(t_o+|t|)f_{11}(2\omega_s|t_o+|t||)\\&+2\Theta(-t_o-|t|)f_{11}(\omega_s(-t_o-|t|))\cos[\omega_s(t-t_o)]\\&-2\Theta(t)\Theta(-t_o-t)f_{11}(\omega_s|2t_o+t|)\cos(\omega_s t)\\&-2\Theta(-t_o)\Theta(t_o+t)f_{11}(\omega_s t)\cos(\omega_s t)\\&+2\Theta(-t_o)\Theta(t_o+t)f_{11}(\omega_s(t+t_o))\cos[\omega_s(t-t_o)]\\&+2\Theta(-t_o)\Theta(t_o+t)f_{11}(\omega_s(t+t_o))\\&\times\cos[\omega_s(t+t_o)]\},\end{aligned} \tag{32}$$

with $t_o=z_0/v$. In Fig. 4 we show these terms as a function of time for the case of a particle of unity charge and velocity $v=10$ a.u. reflecting inside aluminum at two different depths [$z_0=-\pi v/\omega_s$ (full curve) and $z_0=-3\pi v/2\omega_s$ (dashed curve)]. We note that $dW/dt|_B$ is zero while the particle is outside the material. Once inside the solid, the energy-loss rate increases towards its value for an infinite bulk, as given in Eq. (27). However, after the reflection at $t=0$, an oscillatory behavior appears, as discussed in the preceding section. Again, a ''begrenzung'' effect reduces the coupling to bulk plasmons in the vicinity of the surface, and $dW/dt|_B$ approaches zero at $t=|t_o|$. This same ''begrenzung'' increases the coupling to surface plasmons in the vicinity of the surface, and so $dW/dt|_S$ reaches a maximum whenever the particle enters or leaves the solid [Fig. 4(b)]. However, the most interesting feature of these figures is the fact that, when the

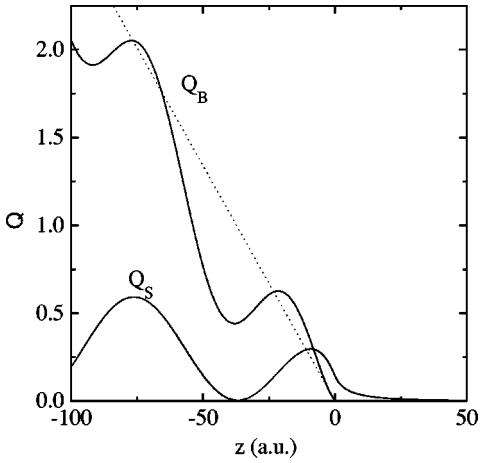

FIG. 5. Functions $Q_B(z)$ and $Q_S(z)$, from Eqs. (33) and (34), giving the average number of bulk- and surface-plasmon excitations in aluminum for normally incident particles, as a function of the coordinate z of the reflection point. The values for $z<0$ correspond to particles reflected inside the metal, while those for $z>0$ (only surface-plasmon excitation) are for particles reflected outside the solid.

particle is reflected at certain characteristic distances from the surface, it can recover in the outgoing part of its trajectory the energy invested in surface-plasmon excitation before the reflection, as in the case shown with dotted line in Fig. 4(b). This striking result can be more clearly seen when the energy-loss rate is integrated in time to get the total energy $\Delta W(z_0)$ dissipated during the reflection process by plasmon excitation.

$$\begin{aligned}\Delta W_B(z_0) &= -\int_{-\infty}^{\infty} \left.\frac{dW}{dt}\right|_B dt \\ &= 2\frac{Z^2\omega_p}{v}\Theta(-t_o)\Big[\omega_p|t_o| f_{11}(0) \\ &\quad - f_{22}(2\omega_p|t_o|) - 2 f_{22}(0) \\ &\quad + \left(\frac{1}{2}f_{11}(0) + f_{21}(0)\right)\sin(2\omega_p|t_o|) \\ &\quad + 4 f_{22}(\omega_p|t_o|)\cos(\omega_p t_o) - f_{22}(0)\cos(2\omega_p t_o)\Big],\end{aligned} \tag{33}$$

$$\begin{aligned}\Delta W_S(z_0) &= -\int_{-\infty}^{\infty} \left.\frac{dW}{dt}\right|_S dt = 2\frac{Z^2\omega_s}{v}\{f_{22}(2\omega_s|t_o|) \\ &\quad + 2\Theta(-t_o) f_{22}(0)[1+\cos(2\omega_s t_o)] \\ &\quad - 4\Theta(-t_o) f_{22}(\omega_s|t_o|)\cos(\omega_s t_o)\}.\end{aligned} \tag{34}$$

In Fig. 5 we show the corresponding average numbers of bulk- and surface-plasmon excitations, defined by $Q_B(z_0) = \Delta W_B(z_0)/\hbar\omega_B$ and $Q_S(z_0) = \Delta W_S(z_0)/\hbar\omega_s$, as a function of the coordinate z_0 of the reflection point. The curves for negative values of z_0 describe those processes where the projectile is reflected inside the solid, while those with $z_0>0$ correspond to a reflection that occurs in the vacuum. In this latter case, $Q_B(z_0)=0$, and $Q_S(z_0)$ decreases when the distance z_0 of closest approach to the surface increases. When the projectile is reflected inside the solid, we note a strong oscillatory behavior of these excitation probabilities as a function of the penetration distance. $Q_S(z_0)$ shows an oscillatory behavior with characteristic wavelength $\pi v/\omega_s$. This effect is dominant for large values of z_0, where Q_S behaves as

$$Q_S(z_0) \approx 4\frac{Z^2}{\hbar v} f_{22}(0)[1+\cos(2\omega_s t_o)]. \tag{35}$$

In particular, we see that $Q_S(z_0)\approx 0$ for certain characteristic depths $z_0=(n+1/2)\pi v/\omega_s$, with $n=0,1,2,\ldots$. The projectile completes its trajectory without any energy loss by surface-plasmon excitation. We should remember, however, the approximation $\gamma=0$ used in this case. For finite values of γ there will be no exact cancellation of the Q_S values. This cancellation effect can be interpreted in terms of the results obtained in the preceding section, where the projectile could recover in one part of its trajectory part of the energy invested in plasmon excitation in another part. $Q_B(z_0)$ also shows a similar oscillatory behavior, superposed to a term linear in the depth z_0 which is related to the mean free path for bulk-plasmon excitation in an infinite medium as discussed in a previous section. The dashed line in Fig. 5 shows the approximation $Q_B(z_0)\approx -2z_0/\lambda_P$, corresponding to Eqs. (27) and (28), where boundary effects are neglected (i.e., the particle is assumed to dissipate energy uniformly, at the bulk rate, once inside the medium).

The oscillatory behavior of $Q(z_0)$ described here was suggested by Ritchie as due to the interference between the incoming and outgoing parts of a reflecting trajectory [17]. It was also described by Yubero and Tougaard [11] and Gervasoni and co-workers [15,16]. However, the present description in terms of energy dissipation rates provides a detailed account of how this interference between the incoming and outgoing trajectories develops in time. Until now, this oscillatory dependence of the energy loss with the depth of penetration in a reflection geometry has not been experimentally investigated, but we may note that a similar effect has been observed in electron bombardment of Ag foils, where the radiation emitted as the result of the decay of plasmons presents an oscillatory dependence with the foil thickness [18], which is also due to interference effects between the incoming and outgoing trajectories.

D. Particle reflected near a metal surface with oblique incidence

Finally, let us consider the case of a particle that is reflected at a distance z from a metal-vacuum interface in a specular trajectory that forms an angle θ with respect to the surface, as shown in Fig. 1. The trajectory reads $\mathbf{R}(t) = (v\ \cos\theta t)\hat{\mathbf{x}} + (v\ \sin\theta|t| + z_0)\hat{\mathbf{z}}$. As before, the reflection occurs inside or outside the material, depending on whether z_0 is negative or positive, respectively.

Let us note that the cylindrical symmetry of the system is lost due to the oblique trajectory. This means that now the energy-loss rates cannot be represented in terms of the simple auxiliary functions f_{nm} as before. In Fig. 6 we show

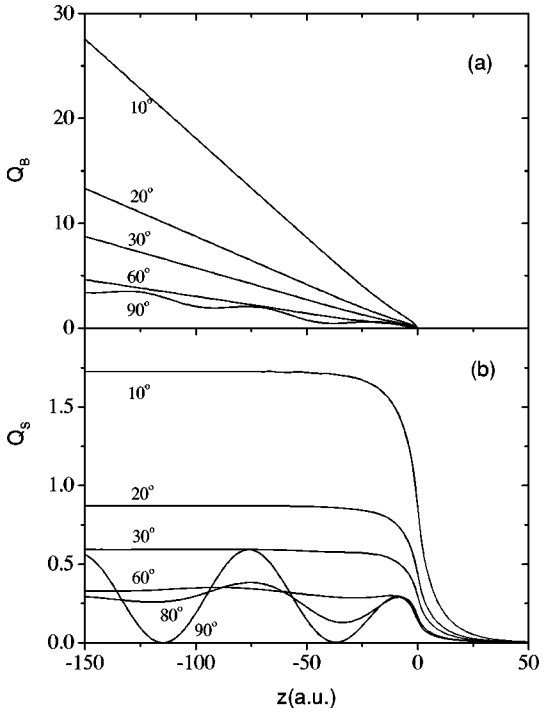

FIG. 6. (a) and (b) show the average number of bulk and surface plasmons, $Q_B(z)$ and $Q_S(z)$, as a function of the coordinate z of the reflection point. The figure corresponds to the case of oblique trajectories, for various angles of incidence θ as indicated in the figure.

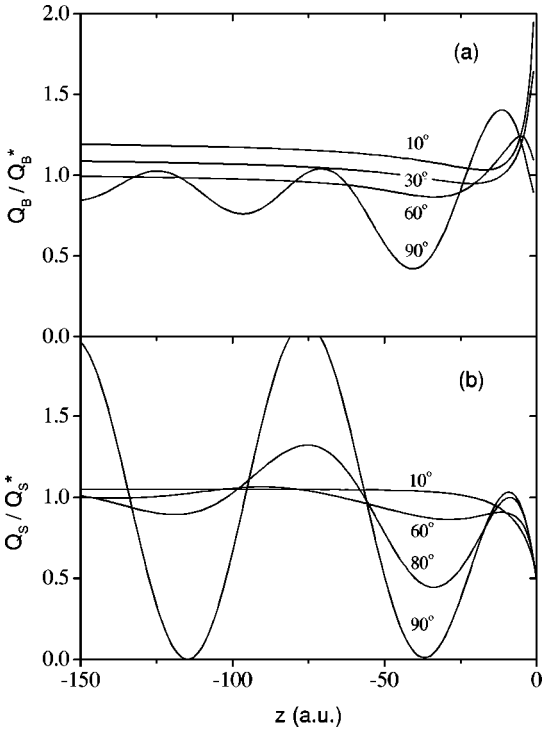

FIG. 7. Average number of bulk and surface plasmons, $Q_B(z)$ and $Q_S(z)$, calculated as in Fig. 6 and normalized to the asymptotic values corresponding to very deep reflection points.

the average numbers of bulk- and surface-plasmon excitations, $Q_B(z)$ and $Q_S(z)$. Again, the curves for negative values of z describe those processes where the projectile is reflected inside the solid, while those with $z>0$ correspond to a reflection that occurs in the vacuum.

As for the case of normal incidence, $Q_B(z_0)=0$ for $z_0>0$, and $Q_S(z_0)$ decreases when the distance z_0 of closest approach to the surface increases. When the projectile is reflected inside the solid, however, we note that the strong oscillatory behavior characteristic of normal incidence disappears at smaller reflection angles θ. In particular, only the term linear in the depth z_0 remains in $Q_B(z_0)$. This term is related to the mean free path λ_P [Eq. (28)] for bulk-plasmon excitation, and increases with the length l traveled by the particle inside the solid. In Fig. 7(a) we show $Q_B(z_0)$ normalized to the average number of bulk-plasmon excitations for a particle traveling a distance $l=2|z_0|/\sin\theta$ inside an infinite solid, given by $Q_B^*(z_0)=l/\lambda_P$. Similarly, Fig. 7(b) shows $Q_S(z_0)$ normalized to twice the average number of surface plasmons excited when a projectile crosses a metal surface in an oblique trajectory, namely, $Q_S^*=2Z^2 f_{22}(0)/\hbar v \sin\theta$ [see Eq. (26)]. The progressive disappearance of the oscillatory contribution, when the angle θ is decreased, is clearly seen in both cases.

Roughly speaking, the oscillatory behavior of $Q(z)$ can be understood as due to the interaction of the emerging projectile with the charge density perturbation produced during its incoming trajectory. Hence, the value of $Q(z)$ would depend on whether the outgoing projectile is in phase or out of phase with these charge density oscillations. However, when surface and bulk plasmons are excited by the particle entering the solid, the charge density is mainly perturbed in the vicinity of the trajectory, up to a distance of the order of $1/q_c$. Thus, after reflection, the projectile would interact strongly with this former perturbation only if it follows a path near to its incoming trajectory. In the present case of oblique incidence, the incident and reflected trajectories do not coincide, and so the oscillatory dependence of $Q(z)$ fades away with decreasing angles θ.

In this example we have used a Drude-type approximation for the dielectric function, as given in Eq. (20). When allowance is made for spatial dispersion through a hydrodynamic dielectric function

$$\varepsilon(k,\omega)=1+\frac{\omega_p^2}{\beta^2k^2-\omega(\omega+i\gamma)}, \tag{36}$$

the plasmon oscillations behave in a different way. The induced potential does not remain localized to the vicinity of the trajectory, but resembles rings of water that spread with velocity $\approx\beta$, leaving behind an oscillating potential plateau [19]. But this perturbation fades away far from the trajectory, and, for particle velocities much larger than the group velocity β (where $\beta\approx 1$ a.u.), the present discussion still applies.

VI. REFLECTION-ELECTRON-ENERGY LOSS

As a final application, let us analyze a beam of electrons reflecting at a metal surface. This problem is of great practical interest in relation with experimental methods where charge projectiles are used as a probe of a solid surface, as in the case of reflection-electron-energy-loss spectroscopy. In principle, for any given REELS geometry the electron can follow different trajectories inside the solid [23,12], which contribute to the measured intensity. Here we shall consider

a simplified model where all the electrons impinge on the surface in an oblique trajectory of angle θ and are specularly reflected by single elastic-scattering events at varying depths z inside the solid. For a monoenergetic beam of electrons of energy E_0, these elastically scattered electrons would be detected roughly around a main spectral line. However, they can lose energy during their travel in and out of the solid by, for instance, plasmon excitations. Thus the spectra would show a series of satellite lines at energies $E_0 - n_B \hbar\omega_p - n_S \hbar\omega_s$, which are due to the excitation of n_B bulk plasmons and n_S surface plasmons. In fact, these are probabilistic processes characterized by Poisson distributions [8,9,20], and an appropriate treatment of these excitations can be obtained from a quantum-mechanical formulation of the processes. This alternative formulation is considered in the Appendix, where we derive the probabilistic distribution of multiple excitations for a beam of electrons. We note, in particular, that, since not all the electrons come from the same depth, these distributions must be averaged over z.

After taking into account the differential probabilities for each trajectory, and integrating over all possible values of penetration distances z, for a beam of electrons incident on the medium, the probability of exciting n_B bulk and n_S surface plasmons finally reads

$$P_{n_B,n_S}(\theta) = \int_{-\infty}^{0} \frac{dz}{\lambda_e \sin\theta} \exp\left(\frac{-2|z|}{\lambda_e \sin\theta}\right) \exp\left(\frac{-2|z|}{\lambda_i \sin\theta}\right) \times P_e(2\theta) \frac{Q_B(z)^{n_B}}{n_B!} \exp[-Q_B(z)] \frac{Q_S(z)^{n_S}}{n_S!} \times \exp[-Q_S(z)]. \quad (37)$$

Here λ_i is the mean free path for all those inelastic processes different from plasmon excitation. The exponential term depending on the elastic mean free path (λ_e) gives the probability that the electron is not elastically scattered in its entire trajectory inside the solid, except at precisely the depth z. This latter collision occurs with a probability $dz/\lambda_e \sin\theta$. Finally, $P_e(\phi)$ is the probability for the electron to be deflected in an angle $\phi = 2\theta$ by this elastic collision with an atom in the solid. We refer to the Appendix for a derivation of this expression and for further details.

Let us now normalize $P_{n_B,n_S}(\theta)$ to the probability $P_{0,0}(\theta)$ for no plasmon excitations, and define the relative-intensity function

$$I_{n_B,n_S}(\theta) = P_{n_B,n_S}(\theta)/P_{0,0}(\theta) = \frac{\int_{-\infty}^{0} dz \exp(-2|z|/\lambda_i \sin\theta) Q_B^{n_B} Q_S^{n_S} \exp(-Q_B - Q_S)}{n_B! n_S! \int_{-\infty}^{0} dz \exp(-2|z|/\lambda_i \sin\theta) \exp(-Q_B - Q_S)}. \quad (38)$$

Since the transport mean free path is much larger for elastic than for inelastic collisions [11,23], in the latter expression we have neglected the exponential term in λ_e.

This integral cannot be evaluated analytically, except if all oscillations and begrenzung effects are neglected. In this latter case, the average number of plasmon excitations can be approximated by their asymptotic values

$$Q_B(z) \approx 2|z|/\lambda_P \sin\theta, \qquad Q_S(z) \approx 2Q_S^0/\sin\theta, \quad (39)$$

where $Q_S^0 = Z^2 f_{22}(0)/\hbar v$ is the average number of surface plasmons excited when a projectile crosses a metal surface in a normal trajectory, as in Eq. (26). Using this approximation in Eq. (38), the normalized probability for the excitation of n_B bulk and n_S surface plasmons becomes

$$I_{n_B,n_S}(\theta) \approx \frac{1}{n_S!} \left(\frac{2Q_S^0}{\sin\theta}\right)^{n_S} \left(\frac{\lambda_i}{\lambda_i + \lambda_P}\right)^{n_B}. \quad (40)$$

Moreover, we see that this expression can be written in terms of the normalized probabilities for excitation of one bulk or one surface plasmon, namely,

$$I_{n_B,n_S}(\theta) \approx \frac{1}{n_S!} [I(0,1)]^{n_S} [I(1,0)]^{n_B}. \quad (41)$$

Equations (40) and (41) provide very useful approximations to evaluate the energy-loss spectra of a beam of electrons in REELS experiments.

In Fig. 8 we show the approximate expressions in Eq. (40) for the relative loss intensities $I(1,0)$ and $I(0,1)$ for the case

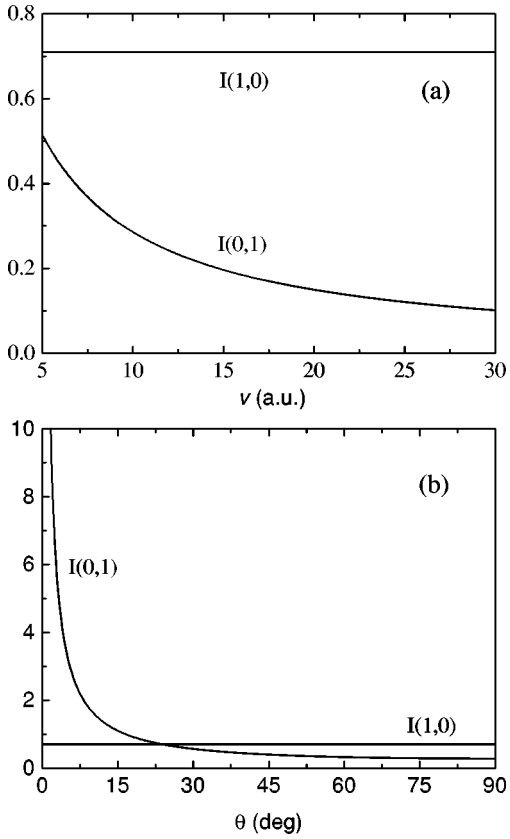

FIG. 8. Approximate expressions for the relative intensities $I(1,0)$ and $I(0,1)$ from Eq. (40), for electrons reflected in aluminum. In (a) we show the velocity dependence for the case of normal incidence, while in (b) we show the angular dependence for a velocity $v = 10$.

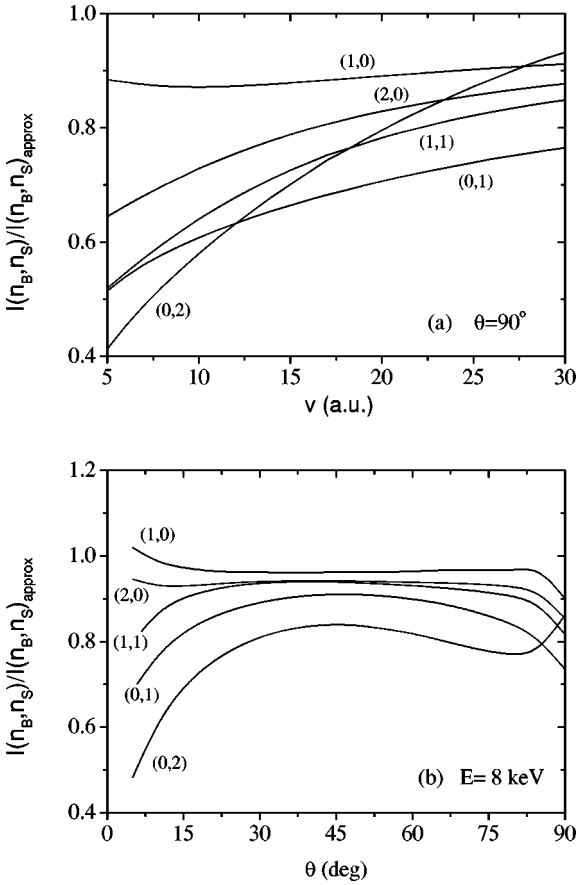

FIG. 9. Relative loss intensities $I(n_P,n_S)$ as given by Eq. (38), normalized to the approximation in Eq. (40), for the reflection of electrons in aluminum; (a) for normal incidence as a function of the electron velocity, and (b) for an electron beam of 8 keV as a function of the angle θ.

of an aluminum surface ($\omega_p = 0.55$ a.u.), showing the dependences on electron velocity v for normal incidence [part (a)], and on incidence angle θ for velocity $v = 10$ [part (b)]. The mean free paths for inelastic collisions λ_i and plasmon excitation λ_P were calculated as indicated by Tung and coworkers [22,23]. We see that the bulk-plasmon excitation probability $I(1,0) \approx \lambda_i/(\lambda_i+\lambda_P)$ is nearly independent of the projectile velocity and incidence angle, whereas the surface-plasmon excitation probability $I(0,1)$ shows a velocity dependence as well as the characteristic angular dependence $\sim 1/\sin\theta$.

These approximate expressions generally overestimate the surface-plasmon excitation probabilities $I(0,n_S)$ and fail for bulk-plasmon production at moderate velocities. This is shown in Fig. 9, where the relative loss intensities $I(n_B,n_S)$ as given by Eq. (38), normalized to the approximation in Eq. (40), are plotted as a function of the electron velocity v for normal incidence (a) and as a function of the angle θ for an electron beam of 8 keV (b). In general, the approximate expressions in Eqs. (40) and (41) worsen for decreasing angles, since ''begrenzung'' effects are comparatively more important. Similarly its failure for decreasing velocities is due to the fact that for not so large velocities the mean free path λ_P for plasmon excitation is comparable to the characteristic distance in the vicinity of the surface where ''begrenzung'' effects are important [14].

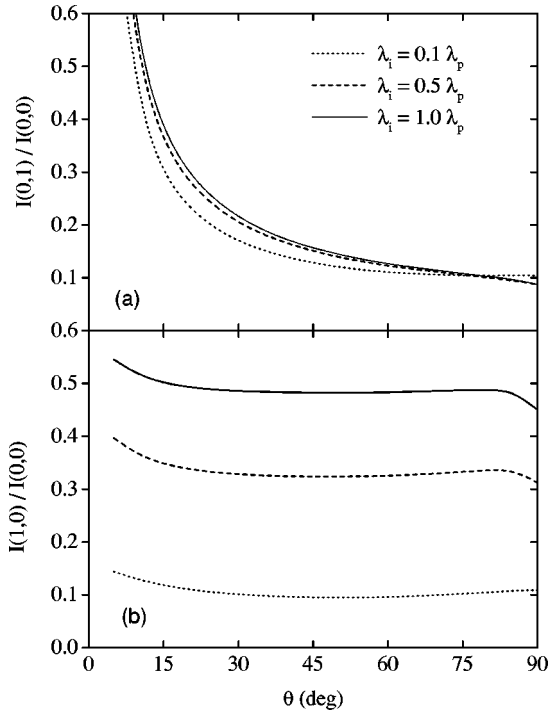

FIG. 10. Mean-free-path dependence of the relative loss intensities $I(n_P,n_S)$, normalized to the intensity of the elastic peak $I(0,0)$, for the reflection of 8-keV electrons in aluminum. We observe that the intensity for bulk plasmons (b) shows a much larger dependence on the λ_i/λ_P value than the one for surface plasmons (a).

From the previous results it seems that one of the relevant parameters in the excitation process is the mean-free-path ratio λ_i/λ_P, showing the relative importance of plasmon excitation versus other excitation processes. The dependence of the relative intensities $I(1,0)/I(0,0)$ and $I(0,1)/I(0,0)$ on this ratio is shown in Fig. 10, for different values of λ_i/λ_P and as a function of the incidence angle θ. We observe that the intensity corresponding to bulk plasmons, $I(1,0)/I(0,0)$ [part (b)], depends very much on the ratio λ_i/λ_P, while its angular dependence is very weak; on the other hand, the intensity corresponding to surface plasmons, $I(0,1)/I(0,0)$ [part (a)], shows a much smaller dependence on λ_i/λ_P, but a large angular dependence.

As a final test of these results, we compare in Fig. 11 the probabilities for the excitation of single bulk or surface plasmons calculated with this model, with the experimental results of Powell [21] for an 8-keV electron beam impinging on an aluminum surface. These experiments provide an important set of data for different angles, showing very nicely the angular dependence of the process. We have adjusted a single free parameter in our model, i.e., the ratio of the plasmon excitation to the inelastic mean free paths $\lambda_P/\lambda_i \approx 2$, so as to fit the bulk-plasmon excitation probability at almost normal incidence. As already indicated, the results for the surface-plasmon excitation are much less sensitive to this ratio, and so similar comparisons can be obtained with slightly different values. In this way we obtain a very satisfactory agreement with the experimental values.

VII. SUMMARY AND CONCLUSIONS

We have formulated in general terms the interaction between a charged particle moving in an arbitrary trajectory

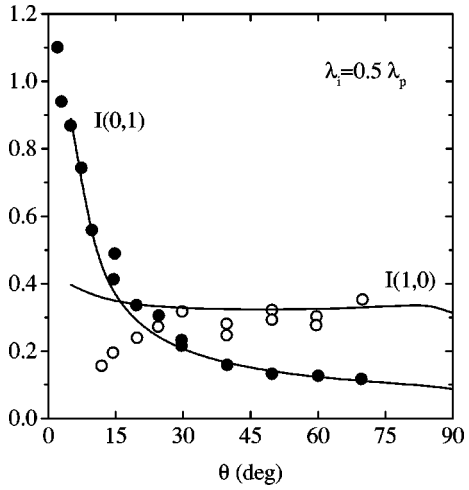

FIG. 11. Probabilities of bulk- and surface-plasmon excitations calculated with this model and compared with the experimental results by Powell (Ref. [21]) for 8-keV electrons reflected on aluminum surfaces.

with the collective modes in the bulk and the surface of a semi-infinite medium. The excitation of plasmons is described using both the dielectric and the quantum-mechanical versions of the process. Both descriptions were shown to be equivalent when a simple plasmon-pole representation of the dielectric function is used. Previous results for simple trajectories may be derived from the present description.

We find that for penetrating trajectories the average number of excited plasmons displays an interference structure which is more important for normal incidence, and gradually diminishes when the incidence angle decreases. The interpretation of this behavior is clear from the present description, and is due to the spatial localization of the induced potential on the surface, both at the penetration and emergence points.

We analyzed in particular the case of electrons reflected in a solid sample and derive expressions for the probability of multiple plasmon excitations by an electron reflected in a specular trajectory. This case is of particular interest for reflection-energy-loss spectroscopies. We may note that other cases of nonspecular-reflection conditions may also be analyzed by a simple extension of the present calculation.

In order to represent the experimental conditions we performed statistical averages that take into account various probability factors: the probability of reflection at various depths inside the medium, the probability of multiple bulk- and surface-plasmon excitations, and the extinction effect due to other inelastic processes. Simple approximations to the complete expressions [like Eqs. (40) and (41)] may also be useful for a more rapid test of experimental results.

We have compared our calculations with the experimental results by Powell. We find a general good agreement for the intensity of the surface-plasmon excitation lines, and we find that the intensity of the bulk-plasmon lines is a sensitive function of the mean-free-path ratio λ_i/λ_P, which measures the relative importance of plasmon excitation versus other excitation processes. This quantity is in principle calculable from current theories on inelastic scattering and electron mean free paths; therefore we expect that the use of the present description of the process may provide a way to extract from the experiments the most adequate values of this ratio, which would be important for comparisons with *ab initio* calculations of mean free paths of electrons in solids.

ACKNOWLEDGMENTS

We gratefully acknowledge useful comments by F. Yubero and M. Vicanek. This work was partially supported by FONCYT (Argentina). One of us (C.D.) is grateful to Ministerio de Educación y Ciencia (Spain) for financial support.

APPENDIX: THE SEMICLASSICAL FORMALISM

We present here a description of the plasmon excitation process using the semiclassical formalism, originally developed by Lucas and Šunjić [24]. In this formalism the external particle is assumed to follow a classical trajectory, whereas the excitations in the medium (bulk and surface plasmons) are described in a quantum-mechanical way. This allows us to calculate the average number of excited plasmons of a fast charge moving inside a material, following an arbitrarily prescribed trajectory. In principle, the analysis may not coincide with that of the dielectric formalism, but we will see that the results are very similar, and in some cases identical, depending on the dielectric functions used.

1. Surface modes

Let us consider two semi-infinite media with dielectric functions $\varepsilon_1(\omega)$ and $\varepsilon_2(\omega)$, and with plasma frequencies ω_{p1} and ω_{p2}, divided by a flat interface at $z=0$. The condition for the existence of surface modes at the interface, obtained by Ritchie [3], is in general given by $\varepsilon_1(\omega)+\varepsilon_2(\omega)=0$, and in particular, for a metal-vacuum interface, by $\varepsilon_1(\omega)+1=0$. For a simple Drude-type dielectric function, the solution to this equation gives a surface-plasmon frequency $\omega_s=\omega_p/\sqrt{2}$. This gives rise to electrostatic fields, which are solutions of the Laplace equation in each medium, $\nabla^2\phi=0$, except for points on the interface, where the sources of the field are located. The solutions of this problem show an oscillatory behavior on the plane of the surface, but decay exponentially for points away from it.

Hence, the general electrostatic potential may be represented in terms of simple plane-wave modes, with wave vectors $\mathbf{q}$ parallel to the surface (and in the range $0<q<q_c$),

$$\phi(\vec{r},t)=\sum_{\mathbf{q}} A_{\mathbf{q}}(z)e^{i\mathbf{q}\cdot\mathbf{r}}e^{-q|z|}\exp(-i\omega_s t)+\text{c.c.} \quad \text{(A1)}$$

This field may be quantized in the usual way [25], replacing the classical amplitudes $A_{\mathbf{q}}$ and $A_{\mathbf{q}}^*$ in terms of the corresponding annihilation and creation operators $a_{\mathbf{q}}$ and $a_{\mathbf{q}}^\dagger$,

$$A_{\mathbf{q}}\rightarrow\left(\frac{\pi\hbar\omega_s}{qA}\right)^{1/2}a_{\mathbf{q}},$$

$$A_{\mathbf{q}}^*\rightarrow\left(\frac{\pi\hbar\omega_s}{qA}\right)^{1/2}a_{\mathbf{q}}^\dagger, \quad \text{(A2)}$$

where A is the area of the surface. Now each mode represents a surface plasmon with momentum $\hbar\mathbf{q}$ and energy $\hbar\omega_s$.

The Hamiltonian of the pure surface-plasmon field takes the usual form

$$H_S^0 = \sum_{\mathbf{q}} \hbar\omega_s a_{\mathbf{q}}^\dagger a_{\mathbf{q}}, \tag{A3}$$

and the final expression for the quantized potential becomes

$$\phi(\vec{r},t) = \sum_{\mathbf{q}} \left(\frac{\pi\hbar\omega_s}{qA}\right)^{1/2} \exp(-q|z|) \times [a_{\mathbf{q}}\exp(-i\omega_s t)\exp(i\mathbf{q}\cdot\mathbf{r}) + a_{\mathbf{q}}^\dagger \exp(i\omega_s t)\exp(-i\mathbf{q}\cdot\mathbf{r})]. \tag{A4}$$

The electric field $\vec{E}$ and induced charge density ρ may be obtained by simple derivations, in particular, we get

$$\rho(\vec{r},t) = -\frac{1}{4\pi}\nabla^2\phi = \sum_{\mathbf{q}} \frac{qA_{\mathbf{q}}}{2\pi}\exp(-i\omega_s t)\exp(i\mathbf{q}\cdot\mathbf{r})\,\delta(z), \tag{A5}$$

which explicitly shows that the sources of this field are located at the surface $z=0$.

a. Interaction with an external charge

Let us consider an external charge Z that moves in a trajectory $\mathbf{R}(t)$. The interaction with the surface-plasmon field is given by the Hamiltonian term:

$$H_{\rm int}(t) = Z\phi[\mathbf{R}(t)] = \sum_{\mathbf{q}} \left(\frac{\pi Z^2\hbar\omega_s}{qA}\right)^{1/2} \exp[-q|\hat{z}\cdot\mathbf{R}(t)|] \tag{A6}$$

$$\times\{a_{\mathbf{q}}\exp(-i\omega_s t)\exp[i\mathbf{q}\cdot\mathbf{R}(t)] + a_{\mathbf{q}}^\dagger \exp(i\omega_s t)\exp[-i\mathbf{q}\cdot\mathbf{R}(t)]\} \tag{A7}$$

and the total Hamiltonian becomes

$$H = \sum_{\mathbf{q}} \hbar\omega_s a_{\mathbf{q}}^\dagger a_{\mathbf{q}} + \sum_{\mathbf{q}} [f_{\mathbf{q}}(t)a_{\mathbf{q}}e^{-i\omega_s t} + f_{\mathbf{q}}^*(t)a_{\mathbf{q}}^\dagger e^{i\omega_s t}], \tag{A8}$$

with

$$f_{\mathbf{q}}(t) = \left(\frac{\pi Z^2\hbar\omega_s}{qA}\right)^{1/2} \exp[-q|\hat{z}\cdot\mathbf{R}(t)|]\exp[i\mathbf{q}\cdot\mathbf{R}(t)]. \tag{A9}$$

The time evolution of the plasmon-field state may be simply obtained in the interaction picture from the equation

$$i\hbar\frac{\partial\Psi(t)}{\partial t} = H_{\rm int}\Psi(t) = \sum_{\mathbf{q}} [f_{\mathbf{q}}(t)a_{\mathbf{q}}e^{-i\omega_s t} + f_{\mathbf{q}}^*(t)a_{\mathbf{q}}^\dagger e^{i\omega_s t}]\Psi(t). \tag{A10}$$

This shows that $\Psi(t)$ has the form of a coherent state [25],

$$\Psi(t) = \exp\left(-i\sum_{\mathbf{q}} [I_{\mathbf{q}}(t)a_{\mathbf{q}} + I_{\mathbf{q}}^*(t)a_{\mathbf{q}}^\dagger]\right)\Psi(-\infty), \tag{A11}$$

with

$$I_{\mathbf{q}}(t) = \frac{1}{\hbar}\int_{-\infty}^{t} f_{\mathbf{q}}(t')\,\exp(-i\omega_s t')dt', \tag{A12}$$

and where $\Psi(-\infty)$ represents the initial state of the plasmons. We assume that the plasmon field is initially in the ground state, $\Psi(-\infty)=|0\rangle$, where $|0\rangle$ is the state with no excited plasmons.

Developing the equation (A11) in eigenstates $|n_{\mathbf{q}}\rangle$ of the free Hamiltonian H_S^0, Eq. (A3), where $n_{\mathbf{q}}$ denotes the number of (excited) plasmons for a given mode $\mathbf{q}$,

$$|n_{\mathbf{q}}\rangle = \frac{(a_{\mathbf{q}}^\dagger)^n}{\sqrt{n!}}|0\rangle, \tag{A13}$$

one gets [25]

$$\Psi(t) = \prod_{\mathbf{q}} \exp\left(-\frac{1}{2}|I_{\mathbf{q}}(t)|^2\right)\sum_{n=0}^{\infty}[-iI_{\mathbf{q}}^*(t)]^n\frac{(a_{\mathbf{q}}^\dagger)^n}{n!}|0\rangle. \tag{A14}$$

Then, the final probability that the particle will excite $n_{\mathbf{q}}$ plasmons of a given mode $\mathbf{q}$, after interacting with the medium between times $t=-\infty$ and $t=+\infty$, is given by

$$P_{\mathbf{q}}^n = |\langle n_{\mathbf{q}}|\Psi(\infty)\rangle|^2 = \exp(-Q_{\mathbf{q}})\,\frac{(Q_{\mathbf{q}})^n}{n!}, \tag{A15}$$

with $Q_{\mathbf{q}} = |I_{\mathbf{q}}(\infty)|^2$. This has the form of a Poisson distribution, with $Q_{\mathbf{q}}$ the relevant parameter that gives the average number of surface-plasmon excitations for a given mode $\mathbf{q}$, viz.,

$$\langle N_{\mathbf{q}}\rangle = \sum_n P_{\mathbf{q}}^n n = \exp(-Q_{\mathbf{q}})\sum_n \frac{(Q_{\mathbf{q}})^n}{n!}n = Q_{\mathbf{q}}. \tag{A16}$$

The simplicity of this result is due to the fact that, since the projectile does not modify its energy or its momentum when it excites one plasmon, the probability of exciting another plasmon is independent of the former process. Hence, the composite probability to excite n_1 plasmons of the mode $\mathbf{q}_1$, n_2 plasmons of the mode $\mathbf{q}_2$, and so on, will be given by

$$P(n_1,n_2,\ldots) = \exp(-Q)\prod_{\mathbf{q}} \frac{(Q_{\mathbf{q}})^{n_{\mathbf{q}}}}{n_{\mathbf{q}}!}, \tag{A17}$$

with

$$Q = \sum_{\mathbf{q}} |I_{\mathbf{q}}(\infty)|^2 = \frac{A}{(2\pi)^2}\int d^2\mathbf{q}|I_{\mathbf{q}}(\infty)|^2 \tag{A18}$$

Here we have transformed the sum over modes into an integral in the usual way.

Finally, we can compute the probability to excite a total number of n plasmons (with any arbitrary distribution of excited modes) as follows:

$$P_n=\sum_{n_1,n_2,\ldots}^{n_1+n_2+\cdots=n} P(n_1,n_2,\ldots)=\frac{Q^n}{n!}\exp(-Q). \tag{A19}$$

From this result we can calculate the average number of plasmons excited by the external charge, after its interaction with the surface,

$$\langle N\rangle=\sum_n n\ P_n=\sum_n n\ \frac{Q^n}{n!}\exp(-Q)=Q. \tag{A20}$$

In particular, the probability of exciting only one plasmon (of any mode) is given by

$$P_1=Q\ \exp(-Q), \tag{A21}$$

and the probability of no-plasmon excitation is simply

$$P_0=\exp(-Q). \tag{A22}$$

b. Electrons reflected at a surface in grazing incidence

Let us consider in particular the case of an electron of velocity **v** which is specularly reflected at the surface of a metal. The angle of incidence measured from the plane of the surface is θ. The trajectory is therefore

$$\mathbf{R}(t)=(v\ \cos\ \theta)\ t\hat{x}+(v\ \sin\ \theta)|t|\hat{z}, \tag{A23}$$

where $\hat{x}$ is a versor parallel to the surface.

Replacing this trajectory in the former formulas, we obtain the average number of excited surface plasmons,

$$Q_S=\frac{Z^2\omega_s}{\hbar\pi}\int_0^{2\pi}d\alpha\int_0^{q_c}dq \times\frac{q^2v_z^2}{[(qv\ \sin\ \theta)^2+(\omega_s-qv\ \cos\ \theta\ \cos\ \alpha)^2]^2}. \tag{A24}$$

If the incidence is very grazing, i.e., $v_z=v\ \sin\ \theta$ is very small, we can make the replacement

$$\frac{q^2v_z^2}{[q^2v_z^2+(\omega_s-qv\ \cos\ \theta\ \cos\ \alpha)^2]^2} \rightarrow\frac{\pi}{2qv_z}\ \delta(\omega_s-qv\ \cos\ \theta\ \cos\ \alpha) \tag{A25}$$

for $v_z\rightarrow 0$.

Using this limit, we can integrate and obtain the following expression for Q_S:

$$Q_S\approx\frac{Z^2}{\hbar v\ \sin\ \theta}\arctan\left(\sqrt{\left(\frac{q_cv}{\omega_s}\right)^2-1}\right). \tag{A26}$$

We can see from this equation that, when the incidence becomes more grazing, the average number of excited plasmons increases. In the limit $\theta\rightarrow 0$, Q_S diverges because the electron moves parallel to the surface, exciting an ever increasing number of plasmons.

On the other hand, in the case of normal incidence, $\theta=90°$, we can integrate Eq. (A24) and obtain

$$Q_S=\frac{Z^2}{\hbar v}\left[\arctan\left(\frac{q_cv}{\omega_s}\right)-\frac{(q_cv/\omega_s)}{1+(q_cv/\omega_s)^2}\right] \tag{A27}$$

in agreement with Eq. (26) in the text, showing explicitly the relation between the mean energy loss and the average number of plasmon excitations: $\Delta W_S=\hbar\omega_sQ_S$. (Notice also that the result is the same for transmission and for reflecting trajectories, since the response of the plasmon field is symmetrical for equal perturbations on both sides of the interface.)

2. Bulk modes

The treatment of the bulk modes is analogous to the one of surface plasmons. The average number of bulk plasmons Q_B excited by a charge moving with trajectory $\mathbf{R}(t)$ is

$$Q_B=\frac{V}{4\pi^3}\int_{k_z>0}d^3\vec{k}|I_{\vec{k}}(\infty)|^2, \tag{A28}$$

$$I_{\vec{k}}(\infty)=\frac{1}{\hbar}\int_{-\infty}^{\infty}dt f_{\vec{k}}(t)\exp(-i\omega_pt), \tag{A29}$$

$$f_{\vec{k}}(t)=\left(\frac{4\pi Z^2\hbar\omega_p}{Vk^2}\right)^{1/2}\exp[i\mathbf{q}\cdot\mathbf{R}(t)]\sin[k_z\hat{z}\cdot\mathbf{R}(t)] \times\Theta(-\hat{z}\cdot\mathbf{R}(t)), \tag{A30}$$

where $\vec{k}=\mathbf{q}+k_z\cdot\hat{z}$ is the three-dimensional wave vector of the bulk plasmon, which for convenience is decomposed into parallel ($\mathbf{q}$) and perpendicular ($k_z\hat{z}$) components with respect to the surface. Here V represents the volume of the medium. The Heaviside function $\Theta(-\hat{z}\cdot\mathbf{R}(t))$ indicates that the coupling with the bulk modes takes place only when the particle is inside the medium.

3. Comparison with the dielectric formalism

a. Surface plasmons

Using the semiclassical formalism, the average number of excited plasmons in a portion of trajectory (from $-\infty$ until a given time t) is

$$Q_S(t)=\frac{A}{(2\pi)^2}\int d^2\mathbf{q}|I_{\mathbf{q}}(t)|^2, \tag{A31}$$

where

$$I_{\mathbf{q}}(t)=\frac{1}{\hbar}\int_{-\infty}^{t}dt' f_{\mathbf{q}}(t')e^{-i\omega_st'}. \tag{A32}$$

Using these equations we obtain

$$Q_S(t)=\frac{A}{(2\pi\hbar)^2}\int d^2\mathbf{q}\int_{-\infty}^{t}dt'\int_{-\infty}^{t}dt''f_{\mathbf{q}}(t')f_{\mathbf{q}}^{*}(t'')\times\exp[-i\omega_s(t'-t'')]. \tag{A33}$$

In order to compare with the dielectric formalism, we derive from this an expression for the energy loss per time unit, as follows:

$$\left.\frac{dW}{dt}\right|_S=-\hbar\omega_s\frac{dQ_S(t)}{dt}$$
$$=-\frac{A\omega_s}{(2\pi)^2\hbar}\int d^2\mathbf{q}\int_{-\infty}^{t}dt'\{f_q(t)f_q^{*}(t')\times\exp[-i\omega_s(t-t')]+f_q(t')f_q^{*}(t)\exp[-i\omega_s(t'-t)]\}. \tag{A34}$$

We consider here the general case of a particle moving with an arbitrary trajectory $\mathbf{R}(t)$, then

$$f_{\mathbf{q}}(t)=\left(\frac{\pi Z^2\hbar\omega_s}{qA}\right)^{1/2}\exp[-q|\hat{z}\cdot\mathbf{R}(t)|]\exp[i\mathbf{q}\cdot\mathbf{R}(t)]. \tag{A35}$$

Replacing this in Eq. (A34), and integrating over the angle of $\mathbf{q}$, we obtain

$$\left.\frac{dW}{dt}\right|_S=-Z^2\omega_s^2\int_0^{q_c}dq\int_{-\infty}^{t}dt'\cos[\omega_s(t-t')]\times J_0[q|\mathbf{R}(t)-\mathbf{R}(t')|\sin\varphi]\times\exp[-q|\hat{z}\cdot\mathbf{R}(t)|-q|\hat{z}\cdot\mathbf{R}(t')|], \tag{A36}$$

where φ is the angle between the vector $\mathbf{R}(t)-\mathbf{R}(t')$ and the normal to the surface.

This expression coincides exactly with Eq. (22) of the text, deduced from the dielectric formalism and the specular-reflection model, using a Drude model for the dielectric function, with plasma frequency ω_p and attenuation constant $\gamma=0$.

b. Bulk plasmons

The treatment for the bulk modes is analogous to the previous one for surface plasmons. Replacing

$$f_{\vec{k}}(t)=\left(\frac{4\pi Z^2\hbar\omega_p}{Vk^2}\right)^{1/2}\sin[k_z\hat{z}\cdot\mathbf{R}(t)]\exp[i\mathbf{q}\cdot\mathbf{R}(t)]\times\Theta(-\hat{z}\cdot\mathbf{R}(t)), \tag{A37}$$

in an equation similar to Eq. (A34) for bulk plasmons, and integrating with respect to k_z and to the angle of $\mathbf{q}$, we obtain

$$\left.\frac{dW}{dt}\right|_B=-Z^2\omega_p^2\Theta(-\hat{z}\cdot\mathbf{R}(t))\int_{-\infty}^{t}dt'\int_0^{q_c}dq\times\Theta(-\hat{z}\cdot\mathbf{R}(t'))(\exp\{-q|\hat{z}\cdot[\mathbf{R}(t)-\mathbf{R}(t')]|\}-\exp\{-q|\hat{z}\cdot[\mathbf{R}(t)+\mathbf{R}(t')]|\})\times\cos[\omega_p(t-t')]J_0[q|\mathbf{R}(t)-\mathbf{R}(t')|\sin\varphi], \tag{A38}$$

which corresponds to Eq. (21) of the text in the limit $\gamma\to0$.

Thus we have shown that the quantum formulation of Lucas for plasmon excitations is equivalent to the dielectric formalism using the specular-reflection model and the Drude approximation (with $\gamma=0$), for particles with arbitrary trajectories.

4. Multiple plasmon excitations

In order to compare our model with experimental results, it is necessary to calculate the probability that the projectile excites n_B bulk plasmons and n_S surface plasmons along its trajectory. To formulate this, we first consider the differential probability $P_{\mathrm{ref}}(z)$ that the particle is reflected due to an elastic scattering process at a depth z inside the material (cf. Fig. 1):

$$P_{\mathrm{ref}}(z)=\exp(-x_1/\lambda_e)\frac{dx}{\lambda_e}\exp(-x_2/\lambda_e)=\exp\left(\frac{-2|z|}{\lambda_e\sin(\theta)}\right)\frac{dz}{\lambda_e\sin(\theta)}, \tag{A39}$$

with $x_1=x_2=|z|/\sin\theta$, $dx=dz/\sin\theta$, and where $\lambda_e=1/n\sigma_e$ is the mean free path for elastic scattering of electrons in the material. Equation (A39) combines the probabilities that the particle is not scattered along the incoming and outgoing trajectories (with path lengths x_1 and x_2, respectively), and suffers a single scattering event in the element of trajectory dx.

The probability for the electron to be scattered in the direction of observation within a small solid angle $d\Omega$ is given by

$$P_e=\frac{1}{\sigma_e}\frac{d\sigma_e}{d\Omega}. \tag{A40}$$

Once this trajectory is defined, the probability of exciting n_B bulk plasmons and n_S surface plasmons by the particle is given by the combined Poisson distribution, as in Eq. (A17):

$$D_{n_B,n_S}=\exp(-Q_B)\frac{Q_B^{n_B}}{n_B!}\exp(-Q_S)\frac{Q_S^{n_S}}{n_S!}, \tag{A41}$$

with the values of Q_B and Q_S calculated before.

Moreover, the probability that no other type of inelastic processes occur for this trajectory is given by

$$P_{\mathrm{in}}(z)=\exp\left[\frac{-2|z|}{\lambda_i\sin\theta}\right], \tag{A42}$$

where λ_i is the mean free path corresponding to any other inelastic process different from plasmon excitation.

Then, we can integrate the total probability of exciting (n_B,n_S) plasmons along the whole trajectory, for a particle reflected at a distance $|z|$ from the surface, assuming a single elastic collision, as follows:

$$\frac{dP_{n_B,n_S}(\theta)}{d\Omega}=\frac{1}{\sigma_e}\frac{d\sigma_e}{d\Omega}\int_{-\infty}^{0}\frac{dz}{\lambda_e\sin\theta}\exp\left[\frac{-2|z|}{\sin\theta}\left(\frac{1}{\lambda_i}+\frac{1}{\lambda_e}\right)\right]D_{n_B,n_S}. \tag{A43}$$

In order to compare with the available experimental data, we consider the ratio between the former expression and the probability that the particle is reflected without any plasmon loss (i.e., the elastic peak), which is given by $dP_{0,0}(\theta)/d\Omega$.

Thus we obtain the *intensity ratio* $I(n_B,n_S)$ for a given value of the incidence angle:

$$I_{n_B,n_S}(\theta)=\frac{dP_{n_B,n_S}(\theta)/d\Omega}{dP_{0,0}(\theta)/d\Omega}=\frac{1}{n_B!n_S!}\frac{\int_{-\infty}^{0}dz\,\exp(-2|z|/\lambda_i\sin\theta)Q_B^{n_B}Q_S^{n_S}\exp(-Q_B-Q_S)}{\int_{-\infty}^{0}dz\,\exp(-2|z|/\lambda_i\sin\theta)\exp(-Q_B-Q_S)}, \tag{A44}$$

where $Q_B=Q_B(z)$ and $Q_S=Q_S(z)$, as calculated before.

We note that, in taking this ratio, the dependence on the elastic-scattering cross section σ_e cancels out.

[1] H. Raether, in *Excitations of Plasmons and Interband Transitions by Electrons*, edited by G. Höhler, Springer Tracts in Modern Physics Vol. 88 (Springer, Berlin, 1980).

[2] K. D. Sevier, *Low Energy Electron Spectrometry* (Wiley-Interscience, New York, 1972).

[3] R. H. Ritchie, Phys. Rev. A **106**, 874 (1957).

[4] R. H. Ritchie and A. L. Marusak, Surf. Sci. **4**, 234 (1966).

[5] F. Flores and F. García-Moliner, J. Phys. C **12**, 907 (1979).

[6] T. L. Ferrell, P. M. Echenique, and R. H. Ritchie, Solid State Commun. **32**, 419 (1979).

[7] R. Núñez, P. M. Echenique, and R. H. Ritchie, J. Phys. C **13**, 4229 (1980).

[8] A. A. Lucas and M. Šunjić, Prog. Surf. Sci. **1**, 75 (1972).

[9] G. D. Mahan, Phys. Status Solidi B **55**, 703 (1973).

[10] G. D. Mahan, in *Electron and Ion Spectroscopy of Solids*, edited by L. Fiermans, J. Venik, and W. Dekeyser (Plenum Press, New York, 1978).

[11] F. Yubero and S. Tougaard, Phys. Rev. B **46**, 2486 (1992).

[12] F. Yubero, J. M. Sanz, B. Ramskov, and S. Tougaard, Phys. Rev. B **53**, 9719 (1996); F. Yubero, D. Fujita, B. Ramskov, and S. Tougaard, *ibid.* **53**, 9728 (1996).

[13] J. L. Gervasoni and N. R. Arista, Surf. Sci. **260**, 329 (1992).

[14] J. L. Gervasoni, N. R. Arista, R. O. Barrachina, and A. Gras-Martí, Nucl. Instrum. Methods Phys. Res. B **67**, 659 (1992).

[15] J. L. Gervasoni, Ph.D. thesis, Instituto Balseiro, Bariloche, 1992.

[16] C. D. Denton, J. L. Gervasoni, R. O. Barrachina, and N. R. Arista, J. Phys.: Condens. Matter **5**, A277 (1993).

[17] R. H. Ritchie (private communication).

[18] W. Steinmann, Phys. Status Solidi **28**, 437 (1968).

[19] H. G. Eriksson, B. R. Karlsson, and K. A. I. L. Wijewardena, Phys. Rev. B **31**, 843 (1985).

[20] W. J. Pardee, G. D. Mahan, D. E. Eastman, R. A. Pollak, L. Ley, F. R. McFeely, S. P. Kowalczyk, and D. A. Shirley, Phys. Rev. B **11**, 3614 (1975).

[21] C. J. Powell, Phys. Rev. **175**, 972 (1968).

[22] C. J. Tung and R. H. Ritchie, Phys. Rev. B **16**, 4302 (1977).

[23] C. J. Tung, Y. F. Chen, C. M. Kwei, and T. L. Chou, Phys. Rev. B **49**, 16684 (1994).

[24] A. A. Lucas, Phys. Rev. B **20**, 4990 (1979); A. A. Lucas and M. Šunjić, J. Vac. Sci. Technol. **9**, 725 (1972).

[25] E. Merzbacher, *Quantum Mechanics* (Wiley, New York, 1970).